British Journal of Pharmacology

DOI:10.1111/j.1476-5381.2011.01520.x
www.brjpharmacol.org

RESEARCH PAPER

Involvement of the first transmembrane segment of human α_2-adrenoceptors in the subtype-selective binding of chlorpromazine, spiperone and spiroxatrine

JMM Laurila[1,5], G Wissel[2,3], H Xhaard[3], JO Ruuskanen[1,4], MS Johnson[2] and M Scheinin[1,4]

[1]*Department of Pharmacology, Drug Development and Therapeutics, University of Turku, Turku, Finland,* [2]*Department of Biosciences (Biochemistry), Åbo Akademi University, Turku, Finland,* [3]*Centre for Drug Research, Faculty of Pharmacy, University of Helsinki, Helsinki, Finland,* [4]*Unit of Clinical Pharmacology, Turku University Hospital, Turku, Finland, and* [5]*Drug Discovery Graduate School, University of Turku, Turku, Finland*

Correspondence
Mika Scheinin, Department of Pharmacology, Drug Development and Therapeutics, University of Turku, FI-20014 TURUN YLIOPISTO, Finland.
E-mail: mika.scheinin@utu.fi

Keywords
α_2-adrenoceptor; antagonist docking; first transmembrane domain; G protein-coupled receptor; ligand binding; molecular modelling

Received
22 September 2010
Revised
16 March 2011
Accepted
11 May 2011

BACKGROUND AND PURPOSE

Some large antagonist ligands (ARC239, chlorpromazine, prazosin, spiperone, spiroxatrine) bind to the human α_{2A}-adrenoceptor with 10- to 100-fold lower affinity than to the α_{2B}- and α_{2C}-adrenoceptor subtypes. Previous mutagenesis studies have not explained this subtype selectivity.

EXPERIMENTAL APPROACH

The possible involvement of the extracellular amino terminus and transmembrane domain 1 (TM1) in subtype selectivity was elucidated with eight chimaeric receptors: six where TM1 and the N-terminus were exchanged between the α_2-adrenoceptor subtypes and two where only TM1 was exchanged. Receptors were expressed in CHO cells and tested for ligand binding with nine chemically diverse antagonist ligands. For purposes of interpretation, molecular models of the three human α_2-adrenoceptors were constructed based on the β_2-adrenoceptor crystal structure.

KEY RESULTS

The affinities of three antagonists (spiperone, spiroxatrine and chlorpromazine) were significantly improved by TM1 substitutions of the α_{2A}-adrenoceptor, but reciprocal effects were not seen for chimaeric receptors based on α_{2B}- and α_{2C}-adrenoceptors. Molecular docking of these ligands suggested that binding occurs in the orthosteric ligand binding pocket.

CONCLUSIONS AND IMPLICATIONS

TM1 is involved in determining the low affinity of some antagonist ligands at the human α_{2A}-adrenoceptor. The exact mechanism is not known, but the position of TM1 at a large distance from the binding pocket indicates that TM1 does not participate in specific side-chain interactions with amino acids within the binding pocket of the receptor or with ligands bound therein. Instead, molecular models suggest that TM1 has indirect conformational effects related to the charge distribution or overall shape of the binding pocket.

Abbreviations

B_{max}, receptor density; TM, transmembrane (domain); XL2, second extracellular loop

© 2011 The Authors
British Journal of Pharmacology © 2011 The British Pharmacological Society

Introduction

α_2-Adrenoceptors regulate a wide range of physiological processes in the CNS and in the target organs of peripheral sympathetic innervation (Link *et al.*, 1996; MacMillan *et al.*, 1996; Altman *et al.*, 1999; Hein *et al.*, 1999; Brede *et al.*, 2002). They are therefore potential drug targets with many clinical applications (e.g. in the treatment of elevated blood pressure and intra-ocular pressure, in alleviation of withdrawal symptoms from opioid and alcohol abuse and as anaesthetic adjuvants in intensive care and surgical settings) (Ruffolo and Hieble, 1994; MacDonald *et al.*, 1997). Humans and other mammals have three α_2-adrenoceptor subtypes (α_{2A}, α_{2B} and α_{2C}) encoded by three distinct intronless genes. Among the three receptor subtypes, 175 of 450–461 amino acid residues are conserved (see Figure S1 of the Supporting information). The extent of conservation is greater within the seven transmembrane (TM) domains, and 29 of the 33 amino acids of TM2–TM7 that constitute the membrane-embedded ligand-accessible surface of the three human α_2-adrenoceptors are identical (Xhaard *et al.*, 2005). This structural similarity is reflected in the highly similar ligand binding properties of the three receptor subtypes (Ruuskanen *et al.*, 2005; Xhaard *et al.*, 2005). Nonetheless, their tissue distributions and mechanisms of regulation differ (Eason *et al.*, 1994; Scheinin *et al.*, 1994; MacDonald and Scheinin, 1995; MacDonald *et al.*, 1997; Saunders and Limbird, 1999; Mansouri *et al.*, 2001). All three human α_2-adrenoceptor subtypes bind the endogenous catecholamines adrenaline and noradrenaline with quite similar affinities, while differences have been found in the binding affinities of some synthetic ligands. Current clinically employed α_2-adrenoceptor drugs (e.g. clonidine and dexmedetomidine), however, show only marginal subtype selectivity, which limits their therapeutic usefulness.

Until the year 2007, the structure of bovine rhodopsin (Palczewski *et al.*, 2000) was the closest available structure to serve as a template for adrenoceptor models, but rhodopsin shares only low sequence identity (~21%) with the adrenoceptors. The structures of two close homologues of the α_2-adrenoceptors, the human β_2-adrenoceptor (PDB code 2RH1, Cherezov *et al.*, 2007; Rosenbaum *et al.*, 2007) and the turkey β_1-adrenoceptor (2VT4, Warne *et al.*, 2008), have now been reported. They share, in their TM regions, on average 37–43% identical aligned amino acids with the human α_2-adrenoceptor subtypes (Xhaard *et al.*, 2006). The crystal structures that have been construed for these GPCRs, rhodopsin and β-adrenoceptors, demonstrate that they share the same overall design, having a core structure composed of seven α-helical TM segments. They have a ligand binding cavity mainly defined by amino acid side chains from TM2-TM7, thus placing the ligand binding site within the cell membrane (Cherezov *et al.*, 2007; Rosenbaum *et al.*, 2007). The second extracellular loop (XL2) folds as a β-hairpin and forms a lid over the binding cavity. A disulphide bridge that connects XL2 (Cxl2.50)[1] to TM3 (C3.25) in the structures of rhodopsin and the β-adrenoceptors, as well as in the human A_{2A} adenosine receptor (PDB code 3EML, Jaakola *et al.*, 2008), is highly conserved among all rhodopsin-like GPCRs. In the β-adrenoceptors, XL2 is partly folded as an α-helix and is further stabilized by one additional disulphide bond that is only found in the β-adrenoceptor structures, but not in rhodopsin or in, for example α_2-adrenoceptors (Cherezov *et al.*, 2007; Weis and Kobilka, 2008).

In all types of adrenoceptors (α_1-, α_2- and β-adrenoceptors), a conserved aspartic acid residue located in TM3 (D3.32) provides an anchoring point for the positively charged amine group of agonist ligands (Strader *et al.*, 1987; Wang *et al.*, 1991; Ruffolo and Hieble, 1994; Hein and Kobilka, 1995). S5.42, S/C5.43 and S5.46 in TM5 are involved in hydrogen bond formation with the catechol hydroxyls of catecholamines (e.g. Strader *et al.*, 1989; Peltonen *et al.*, 2003; Xhaard *et al.*, 2006). We have previously mapped the structural determinants of agonist and antagonist binding specificity in the α_2-adrenoceptor subtypes. We employed site-directed mutagenesis, sets of chemically related ligands and sulphydryl-reactive covalently binding ligands in combination with molecular modelling using receptor models based on the bovine rhodopsin structure (Marjamäki *et al.*, 1999; Ruuskanen *et al.*, 2005; Xhaard *et al.*, 2005; Laurila *et al.*, 2007). The main binding site differences among the α_2-adrenoceptor subtypes are located in TM5 and in XL2, where for compounds structurally similar to yohimbine, two residues in XL2 and Cys/Ser^{201} in TM5 (position 5.43) were shown to be major determinants of subtype and species selectivity of ligand binding (Cockcroft *et al.*, 2000; Laurila *et al.*, 2007). However, there is one experimental observation that this model cannot account for; 'bulky' antagonists with an extended, branched and relatively rigid structure, and occupying more volume in comparison to other antagonist ligands, such as ARC239, prazosin, spiperone and spiroxatrine, bind to the human α_{2A}-adrenoceptor with 10- to 100-fold lower affinity than to the α_{2B} and α_{2C} subtypes, and differences in TM5 and XL2 do not explain these affinity differences (Cockcroft *et al.*, 2000; Frang *et al.*, 2001; Laurila *et al.*, 2007).

Since the orthosteric binding cavity of α_2-adrenoceptors has already been quite extensively explored by targeted mutagenesis, we decided to search for determinants of antagonist binding specificity from other regions of the protein structures, in particular TM1, which is the most variable of the seven TMs, with only ~30% sequence identity shared across the α_2-adrenoceptor subtypes in comparison with 60–80% for the other TMs. We made eight chimaeric α_2-adrenoceptor constructs where TM1 was exchanged either with or without the preceding N-terminal sequence. We tested these constructs with nine antagonist ligands. As a result, we showed that TM1 is involved in defining the specific pharmacological profile of the human α_{2A}-adrenoceptor. The exact mechanism of this influence is yet to be characterized, but molecular modelling based on the crystal structure of the human β_2-adrenoceptor

[1]Amino acid residues in GPCRs are numbered according to the Ballesteros–Weinstein nomenclature (Ballesteros and Weinstein, 1995). In this indexing system, the first number refers to the transmembrane helix where the residue is located and the number after the decimal point refers to the residue position with respect to the most conserved residue in that helix, which has been arbitrarily assigned the number 50. In addition, the Ballesteros–Weinstein numbering scheme was extended to the second extracellular loop; thus, the conserved cysteine in XL2 that forms a disulphide bond in all rhodopsin-like GPCRs is indicated as Cxl2.50 (Xhaard *et al.*, 2005).

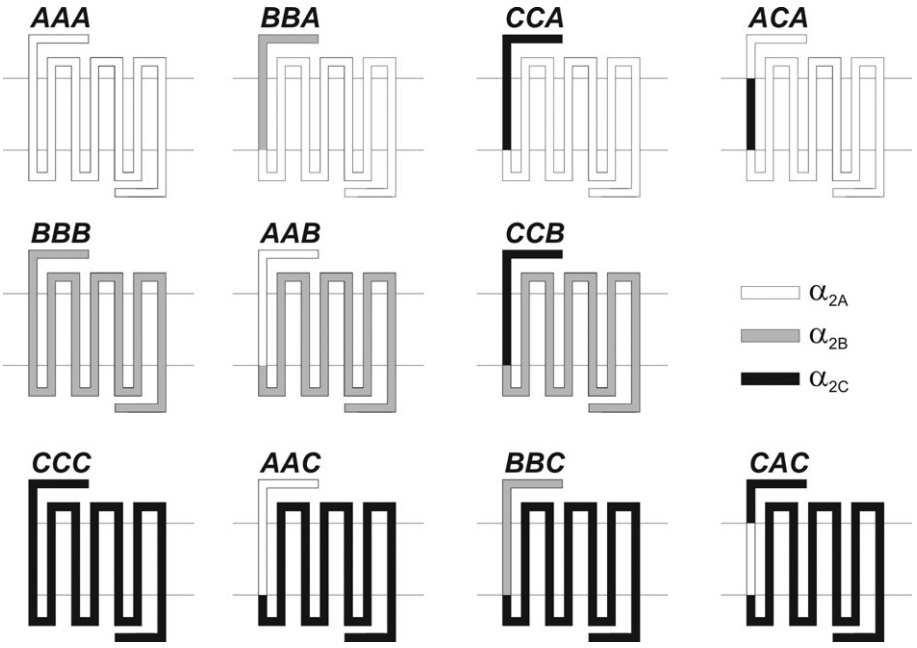

Figure 1

Schematic presentation of chimaeric receptor constructs. Sequences of the wild-type human α_{2A}-adrenoceptor, wild-type human α_{2B}-adrenoceptor and wild-type human α_{2C}-adrenoceptor are shown. Receptors are named based on the origin of the sequence of the N-terminal segment, the TM1 domain and the body of the receptor [e.g. (BBA) for the human α_{2A}-adrenoceptor containing the N-terminal segment and TM1 of the human α_{2B}-adrenoceptor].

(Cherezov *et al.*, 2007; Rosenbaum *et al.*, 2007) suggests that indirect effects are likely to be involved.

Methods

Drugs and other materials

cDNAs encoding the human α_{2A}-, α_{2B}- and α_{2C}-adrenoceptors were originally provided by Dr BK Kobilka (Stanford University, CA). Primers for DNA construction and sequencing were obtained from TAG Copenhagen A/S (Copenhagen, Denmark). [^{3}H]-RX821002 (1,4-[6,7(n)-^{3}H]benzodioxan-2-methoxy-2-yl)-2-imidazoline), specific radioactivity 58 Ci·mmol^{-1}, was purchased from Amersham Pharmacia Biotech (Buckinghamshire, UK). ARC239 was purchased from Tocris (Bristol, UK). Atipamezole was a gift from Orion Pharma (Turku, Finland). Clozapine, chlorpromazine, idazoxan, oxymetazoline, prazosin, spiperone and spiroxatrine were purchased from Sigma-Aldrich (St. Louis, MO). Fetal bovine serum was from Autogen Bioclear UK Ltd. (Wiltshire, UK). Cell culture reagents were supplied by Life Technologies, Inc. (Rockville, MD). Geneticin (G418 disulphate salt solution), hygromycin B, penicillin, streptomycin, trypsin and bovine serum albumin were purchased from Sigma-Aldrich. Other reagents were of analytical or reagent grade and were purchased from commercial suppliers.

DNA constructs and expression vectors

Eight receptor chimaeras were constructed (Figure 1). The wild-type cDNAs were cloned into pREP4 (α_{2A} and α_{2B}) or pcDNA3 (α_{2C}) expression vectors (Invitrogen Life Technologies, Inc., Rockville, MD). Receptor chimaeras were built utilizing a conserved threonine–serine site at the intracellular end of TM1. Chimaeras based on the α_{2A}- and α_{2B}-adrenoceptors were constructed using PCR and two pairs of primers designed for each subtype: a forward primer from the N-terminus of the receptor and a reverse primer until the end of TM1 (containing an artificial *Spe*I site; recognition sequence ACTAGT, coding for TS); a forward primer from the start of the first intracellular loop (also containing an artificial *Spe*I site) and a reverse primer until the C-terminus. In addition, the N- and C-terminal primers contained restriction sites for subcloning into the pREP4 expression vector. Fragments were PCR-amplified, digested and ligated into pREP4 for expression in mammalian cells.

Chimaeras based on the α_{2C}-adrenoceptor were constructed using the Gene Editor™ *in vitro* Site-Directed Mutagenesis System (Promega, Madison, WI); the nucleotide sequence encoding the threonine and serine residues at the end of TM1 was mutated to contain an *Spe*I site. Subsequently, the α_{2C}-adrenoceptor-based chimaeras were constructed using the artificial *Spe*I site and PCR-amplified TM1 (and N-terminal) fragments of the α_{2A}- and α_{2B}-adrenoceptors, and the digested fragments were ligated and subcloned into the pcDNA3.1(+) expression vector.

The α_{2A}- and α_{2C}-adrenoceptor chimaeras with only TM1-region substitutions were constructed with the GeneEditor™ *in vitro* Site-Directed Mutagenesis System and the previous chimaeras as templates; the nucleotide sequence coding for the conserved tyrosine-serine pair at the end of the N-terminus was mutated to contain an *Nhe*I site (recognition sequence

GCTAGC, coding AS). Subsequently, using this artificial *Nhe*I site, the N-terminal fragments were digested, isolated from agarose gel and ligated to the appropriate α_{2A}- and α_{2C}-adrenoceptor-based chimaeras. Thereafter, the artificial *Nhe*I sites were restored to contain the original tyrosine–serine pair.

Cell culture and transfections

All plasmid DNA constructs were sequenced with vector- and gene-specific primers in order to confirm the successful construction of the desired chimaeras and to exclude undesired mutations. Adherent CHO cells (K1 strain) (American Type Culture Collection, Manassas, VA) were transfected and cultured as reported previously (Laurila *et al.*, 2007). Briefly, cells were cultured in α-MEM medium (α-Minimum Essential Medium, Gibco™, Invitrogen, Carlsbad, CA) supplemented with 26 mM $NaHCO_3$, 50 IU·mL^{-1} penicillin, 50 µg·mL^{-1} streptomycin and 5% heat-inactivated fetal bovine serum supplemented with the appropriate selection antibiotic. Cells were grown in a humidified 5% CO_2 atmosphere at 37°C. Stable cell lines expressing the wild-type cDNAs encoding human α_{2A}-, α_{2B}- and α_{2C}-adrenoceptor subtypes were produced previously by Pohjanoksa *et al.* (1997) using the expression vector pMAMneo (Clontech, Palo Alto, CA) that contains a neomysin analogue (Geneticin®, G418) resistance gene. The chimaeric pREP4-based receptor constructs were transfected into CHO cells using the commercial Lipofectamine 2000 kit (Invitrogen), whereas the pcDNA3-based expression constructs were transfected with the FuGENE® HD Transfection Reagent kit (Roche Applied Science, Indianapolis, IN). Transfection mixtures were prepared in serum- and antibiotic-free α-MEM and contained 1–5 µg of plasmid DNA. After 24 h incubation, the pREP4-based transfected cell cultures were expanded using hygromycin B (600 µg·mL^{-1}), and the pcDNA3-based transfections were expanded using G418 (800 µg·mL^{-1}) for selection. The resulting cell cultures were screened for their capacity to bind the α_2-adrenoceptor antagonist radioligand [^{3}H]-RX821002 (see below). Cell cultures with the highest levels of receptor expression were chosen for further experiments and were maintained in 200 µg·mL^{-1} of the appropriate selection antibiotic.

Cells transfected with the α_{2C}-adrenoceptor-based plasmid construct containing TM1 and the N-terminus from the α_{2B}-adrenoceptor failed to show [^{3}H]-RX821002 binding in spite of several transfection experiments with several batches of plasmid DNA. Total RNA was isolated from transfected, antibiotic-resistant CHO cells and converted to cDNA with the DyNAmo™ cDNA Synthesis kit (FinnZymes, Espoo, Finland). PCR amplification was performed with gene-specific primers (see the Supporting information, Figure S2), and control reactions were run using RNA from non-transfected cells.

Membrane preparations

Cell membranes were prepared as described previously (Pohjanoksa *et al.*, 1997) and stored at −78°C. Protein concentrations were determined with the method of Bradford (1976) with BSA as a reference.

Saturation binding assays

Receptor expression levels were determined with saturation binding experiments as described previously (Halme *et al.*, 1995) with [^{3}H]-RX821002 as radioligand. Cell membranes (5–10 µg protein) were incubated with serial dilutions (0.0625–8 nM) of the radioligand. Bound radioactivity was measured with a Wallac 1410 liquid scintillation counter (Perkin-Elmer Wallac, Turku, Finland). Non-specific binding was defined in parallel tubes with an excess of phentolamine (10 µM). Specific binding was defined as the difference between total and non-specific binding. Saturation binding experiments were performed in triplicate and repeated at least three times for each receptor type. Receptor densities (B_{max}) and equilibrium dissociation constants (K_d) were calculated with GraphPad Prism 4.0 software (San Diego, CA).

Competition binding assays

Competition binding assays were implemented using a MultiScreen Vacuum Manifold system (Millipore Corporation, Bedford, MA) with Millipore MultiScreen MSFBN 96-well glass fibre filtration plates. The experiments were performed in a total assay volume of 180 µL (in 50 mM potassium phosphate buffer, pH 7.4) using [^{3}H]-RX821002 at concentrations close to its K_d for each receptor variant, six to eight serial dilutions of the competitor ligands and membrane preparations containing 2–10 µg of protein per sample. Non-specific binding was determined in parallel wells in the presence of 100 µM oxymetazoline. Bound radioactivity was measured with a Wallac 1450 MicroBeta scintillation counter.

Nine antagonist ligands were chosen for the competition binding assays on the basis of their chemical diversity: four 'bulky' antagonists (ARC239, prazosin, spiperone, spiroxatrine), two imidazoles (atipamezole, idazoxan), two tricyclic antipsychotic drugs (chlorpromazine, clozapine) and the yohimbine stereoisomer rauwolscine. The apparent affinity (apparent K_i) of each ligand was determined using nonlinear regression analysis (GraphPad Prism), assuming one-site binding. For conversion of IC_{50} estimates to K_i values, the Cheng–Prusoff equation was applied (Cheng and Prusoff, 1973). The statistical significance of differences between the chimaeras and the corresponding wild-type receptors was evaluated with unpaired *t*-tests.

Sequence alignments, molecular modelling, docking simulations

Molecular models of the α_2-adrenoceptor subtypes were constructed using the software Modeller 8v2 (Sali and Blundell, 1993) as described previously (Xhaard *et al.*, 2005), but using the 2.4 Å β_2-adrenoceptor structure (PDB code 2RH1; Cherezov *et al.*, 2007) as the template. First, pairwise sequence alignments of the human β_2-adrenoceptor sequence with the amino acid sequences of each of the three human α_2-adrenoceptor subtypes were constructed using Malign (Johnson and Overington, 1993). Regions that were too dissimilar to be aligned (i.e. the N-terminal segment and the third intracellular loop) were deleted from the alignments and were not included in the models. During the modelling procedure, the sequence alignments were modified in order to ensure that the conformation of the second extracellular loop (XL2), as built by Modeller 8v2, was relaxed and free of any undesirable atomic contacts. A multiple sequence alignment that contains the three pairwise alignments used for modelling is shown in Figure 2. Ten models were constructed

Figure 2

Multiple sequence alignment of the three human α_2-adrenoceptor subtypes together with the human β_2-adrenoceptor sequence as found in the PDB structure 2RH1. α-helices in the human β_2-adrenoceptor are shown as cylinders above the alignment. Stars (*) indicate amino acids that are located less than 4.5 Å away from the ligands bound to each structure (carazolol in the β_2-adrenoceptor) and indicate the location of the ligand binding sites. Positions conserved amongst the aligned sequences are shaded in grey (dark grey: four receptors; light grey: three receptors). Regions with small letters could not be aligned reliably. The third intracellular loop is not shown for clarity.

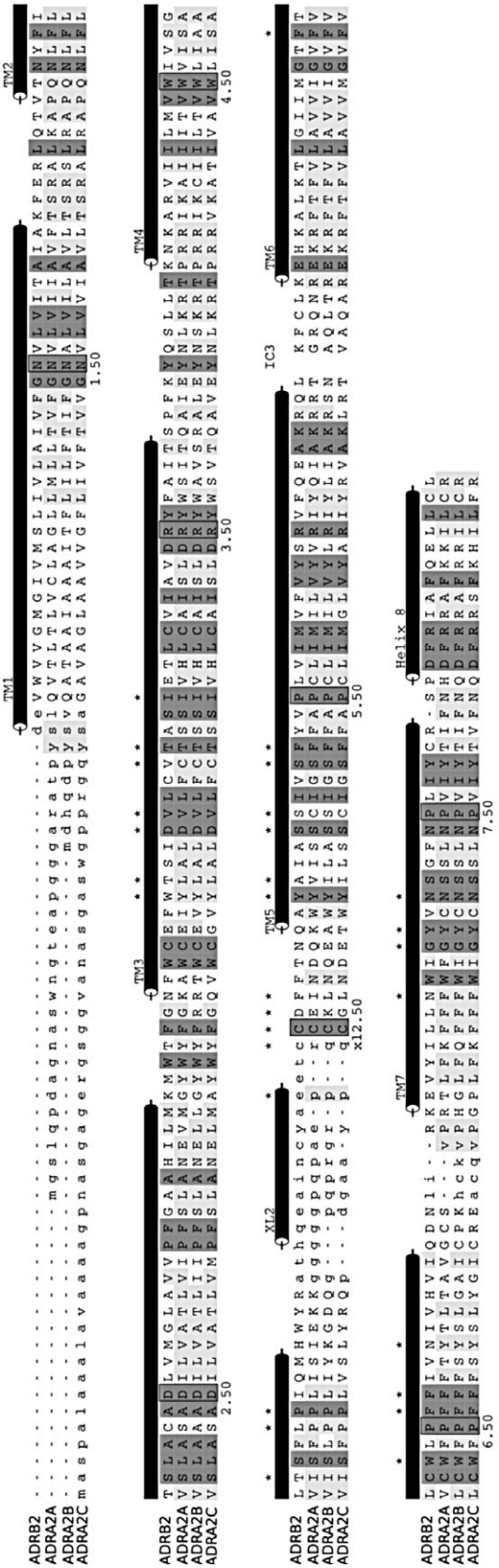

for each of the receptor subtypes that varied in the conformations adopted by their side chains and represented the space accessible to the software Modeller (see Xhaard *et al.*, 2005).

For molecular docking simulations, we selected only the three 'bulky' ligands for which exchange of TM1 had an experimental effect (spiperone, spiroxatrine and chlorpromazine), as well as rauwolscine for which comprehensive mutagenesis-derived information is available (Laurila *et al.*, 2007). The three-dimensional models of the four ligands were prepared as reported previously (Xhaard *et al.*, 2005), with protonation of their central nitrogen atom. Docking was performed using Gold v4.0 (Jones *et al.*, 1997), a programme that allows flexibility in the ligands. Docking simulations were performed with 10 protein models for each of the three receptor subtypes in order to approximate the flexibility of the binding site. Individually for each model and each ligand, 10 docking runs were allowed. The top-ranking structure was further considered. The centre of the search space was taken as an oxygen atom of the conserved D3.32 with a radius of 10 Å around it. The models were ranked in comparison with carazolol bound to the β_2-adrenoceptor crystal structure (Cherezov *et al.*, 2007), by computing a shape and electrostatic overlap index using the programme ShaEP (Vainio *et al.*, 2009).

Results

The N-terminus and TM1 are highly variable regions

We constructed eight chimaeric α_2-adrenoceptors, initially exchanging between the human α_2-adrenoceptor subtypes both the N-terminus and TM1 (subsequently referred to as N_{ter}-TM1), and later only TM1. Seven of the constructs were successfully expressed and then tested along with the three wild-type receptors against a panel of nine antagonist ligands. TM1 is much more variable than the other six TMs, which is shown in the alignment of the α_2-adrenoceptor subtype sequences presented in Figure 2: of the 29 residues aligned with TM1 of the human β_2-adrenoceptor, in the α_2-adrenoceptors 17 differ between subtypes A and B, 18 differ between A and C and 14 differ between B and C. As seen in the sequence alignment, the length of the N-terminus (until the cut-off used in this study, between Y1.28 and S1.29) differs notably between the α_2-adrenoceptor subtypes, con-

Table 1

Binding affinities of [^{3}H]RX821002 and receptor densities in recombinant CHO cell lines (means ± SEM)

Receptor	K_d (nM)	B_{max} (fmol·mg^{-1})
α_{2A} *AAA*	0.45 ± 0.04	6 700 ± 100
α_{2A} *BBA*	1.2 ± 0.7	400 ± 260
α_{2A} *CCA*	0.39 ± 0.06	5 600 ± 500
α_{2A} *ACA*	0.27 ± 0.02*	19 000 ± 3000
α_{2B} *BBB*	4.6 ± 1.0	1 500 ± 300
α_{2B} *AAB*	1.4 ± 0.1*	1 600 ± 100
α_{2B} *CCB*	1.6 ± 0.2*	6 100 ± 500
α_{2C} *CCC*	0.87 ± 0.06	1 800 ± 0
α_{2C} *AAC*	0.71 ± 0.04	470 ± 10
α_{2C} *BBC*	n.d.	n.d.
α_{2C} *CAC*	0.55 ± 0.15	710 ± 80

Receptors are named based on the exchanged domains (see Figure 1). Statistical significance of differences between the chimaeric receptors and the respective wild-type receptors were tested with Student's *t*-test: *$P < 0.05$.
Abbreviations: A (α_{2A}); B (α_{2B}); C (α_{2C}); n.d., not determined.

sisting of 28, 7 and 46 amino acids in subtypes A, B and C, respectively. Thus, any structural model of the N_{ter}-TM1 region is highly speculative, since reliable templates to model the N-terminal segment of each receptor subtype are lacking.

The following eight chimaeras were generated and expressed in CHO cells: each of the subtypes A, B and C with the N_{ter}-TM1 segments of the other two subtypes (six constructs), and the A and C subtypes with TM1 of the C and A subtypes (two constructs). These exchanges took advantage of a conserved tyrosine–serine pair at the end of the N-terminal region and a conserved threonine–serine pair at the end of TM1.

Expression of receptor chimaeras

All chimaeras, with the exception of the α_{2C}-adrenoceptor-based construct that contained N_{ter}-TM1 from the α_{2B}-adrenoceptor, were successfully expressed in CHO cells and displayed only relatively small differences in their affinity for the radioligand [^{3}H]-RX821002 in comparison with the corresponding wild-type receptor (Table 1). For the wild-type receptors, [^{3}H]-RX821002 showed lower affinity at the human α_{2B}-adrenoceptor subtype as compared with the A and C subtypes; this 5- to 10-fold affinity difference agrees with previous findings (Deupree *et al.*, 1996; Uhlén *et al.*, 1998). After introduction of the N_{ter}-TM1 region of the A or C subtype into the α_{2B}-adrenoceptor subtype, [^{3}H]-RX821002 was bound with threefold higher affinity to both α_{2B}-based chimaeras in comparison with the wild-type receptor, shifting the affinity towards that of the wild-type A and C subtypes. Cells transfected with the α_{2A}-based construct containing N_{ter}-TM1 of the B subtype showed a reciprocal effect, with an almost threefold decrease in affinity relative to the A subtype (i.e. a shift towards that of the wild-type B subtype). With the α_{2C}-adrenoceptor-based construct containing N_{ter}-TM1 from the α_{2B}-adrenoceptor, binding of [^{3}H]-RX821002 was not detectable, even if the successful transfection of the chimaeric cDNA was confirmed by reverse transcription PCR (results not shown).

Characterization of antagonist binding profiles

The binding affinities of the antagonist ligands ARC239, prazosin, spiperone, spiroxatrine, chlorpromazine, atipamezole, idazoxan, clozapine and rauwolscine at the different receptor chimaeras and wild-type α_2-adrenoceptors are shown in Table 2. Five ligands (ARC239, prazosin, spiperone, spiroxatrine and chlorpromazine) showed significantly lower affinity for the A subtype in comparison to the B and C subtypes, as evidenced by 10- to 100-fold differences in the binding affinities. The other antagonists did not show significant subtype selectivity between the wild-type receptors and were therefore used as controls.

In the chimaeric receptor based on the α_{2A}-adrenoceptor where N_{ter}-TM1 of the B subtype had been inserted, the binding affinities were significantly improved for two ligands (spiroxatrine and chlorpromazine), and in the case of the insertion of N_{ter}-TM1 from the C subtype into the α_{2A}-adrenoceptor, the binding affinities of three ligands (spiperone, spiroxatrine and chlorpromazine) were significantly improved in comparison with the corresponding wild-type receptor. Similar tendencies were also seen for ARC239 and prazosin, but they failed to reach statistical significance. In order to see which region of N_{ter}-TM1 was responsible for the improved affinity, we created an α_{2A}-adrenoceptor construct where only TM1 had been imported from the C subtype and the original N-terminus of the α_{2A}-adrenoceptor was retained. The binding affinities did not differ between this TM1-only chimaera and the previous N_{ter}-TM1 chimaera, pointing to the involvement of TM1 in the observed binding affinity changes.

In chimaeras based on α_{2B}- and α_{2C}-adrenoceptors and containing N_{ter}-TM1 from the A subtype, or the α_{2C}-adrenoceptor chimaera with only TM1 of the A subtype, no significant changes in ligand affinities were observed. Insertion of N_{ter}-TM1 from the C subtype into the α_{2B}-adrenoceptor did not result in notable differences in the binding affinities.

The β_2-adrenoceptor structure as template for α_2-adrenoceptor models

Our previous α_2-adrenoceptor models (Ruuskanen *et al.*, 2004; Xhaard *et al.*, 2005; 2006; Laurila *et al.*, 2007) were based on the X-ray structure of bovine rhodopsin (Palczewski *et al.*, 2000), but these proteins share only 20–23% sequence identity in their TM regions. The recently reported structures of the turkey β_1-adrenoceptor and the human β_2-adrenoceptor, unlike rhodopsin, share with the α_2-adrenoceptors both higher levels of sequence identity – 37–43% in the TM regions – and higher similarity of some specific amino acid residues shown by other methods to be involved in the recognition of catecholamines (Xhaard *et al.*, 2006). The β_2-adrenoceptor structure (2.4 Å resolution; Cherezov *et al.*, 2007), closely related in evolution to the α_2-adrenoceptors, is therefore likely to allow construction of

Table 2

Competition binding affinities of different ligands obtained with [^{3}H]RX821002 at wild-type and chimaeric α_2-adrenoceptors expressed in CHO cells

Ligand	WT (AAA)	n_H	Human α_{2A} BBA	n_H	CCA	n_H	ACA	n_H
ARC239	1600 (1000–2600)	0.89	450 (160–1400)	0.66	820 (600–1110)	0.72	760 (480–1200)	1.02
Prazosin	1500 (800–3100)	0.84	1400 (490–2400)	1.16	820 (600–1100)	0.94	910 (600–1500)	0.89
Spiperone	1200 (870–1600)	0.94	870 (450–1800)	0.93	560 (440–730)[a]	1.03	500 (320–770)[aa]	0.86
Spiroxatrine	550 (240–1300)	1.33	69 (34–140)[aa]	0.92	71 (39–130)[aa]	1.08	91 (48–180)[aa]	1.51
Chlorpromazine	600 (430–870)	0.82	160 (83–310)[aaa]	0.89	120 (56–260)[aaa]	0.68	160 (100–230)[aaa]	1.07
Clozapine	89 (54–150)	0.91	67 (32–150)	0.69	34 (17–67)	0.58	51 (35–77)	1.13
Atipamezole	2.1 (1.5–3.1)	0.89	2.0 (0.99–4.3)	1.00	1.2 (0.95–1.5)	0.82	1.1 (0.77–1.5)	0.97
Idazoxan	22 (15–31)	0.80	15 (2.7–45)	0.97	17 (13–24)	0.91	13 (8.3–22)	0.85
Rauwolscine	1.8 (0.78–4.5)	0.53	4.4 (2.0–9.8)	0.66	0.85 (0.40–2.1)	1.02	1.6 (0.82–3.1)	0.71

Ligand	WT (BBB)	n_H	Human α_{2B} AAB	n_H	CCB	n_H
ARC239	150 (40–570)[bbb]	0.74	240 (120–480)	0.72	98 (48–220)	0.74
Prazosin	47 (17–140)[bb]	0.79	200 (120–360)	0.82	170 (89–310)	0.89
Spiperone	12 (3.7–38)[bbb]	0.51	26 (11–65)	1.65	14 (6.0–38)	0.67
Spiroxatrine	2.4 (1.2–5.0)[bbb/cc]	0.64	6.8 (1.8–28)	2.03	1.6 (0.64–5.9)	0.91
Chlorpromazine	43 (20–100)[bbb/cc]	0.64	53 (20–200)	1.84	46 (18–120)	0.70
Clozapine	12 (5.0–28)[bbb]	0.93	18 (8.7–45)	1.09	6.7 (1.9–23)	0.64
Atipamezole	2.7 (0.56–14)	0.85	3.0 (1.7–5.6)	0.86	1.7 (0.80–4.0)	0.65
Idazoxan	24 (18–34)	1.08	37 (29–48)	0.95	30 (19–51)	0.88
Rauwolscine	1.1 (0.7–1.8)	0.97	1.2 (0.66–2.4)	1.25	2.7 (1.1–6.9)	1.02

Ligand	WT (CCC)	n_H	Human α_{2C} AAC	n_H	BBC	CAC	n_H
ARC239	130 (66–260)[ddd]	1.15	180 (86–380)	0.89	n.d.	77 (34–180)	0.65
Prazosin	45 (21–81)[dd]	0.67	110 (50–230)	0.78	n.d.	120 (55–260)	0.56
Spiperone	29 (9.2–81)[ddd]	0.66	26 (10–75)	0.63	n.d.	39 (18–89)	0.79
Spiroxatrine	13 (5.9–28)[ddd]	1.13	12 (5.8–27)	1.05	n.d.	18 (8.4–31)	0.68
Chlorpromazine	260 (150–350)[dd]	0.81	260 (110–720)	0.42	n.d.	230 (130–400)	0.80
Clozapine	6.5 (2.5–18)[ddd]	0.75	5.1 (2.6–8.2)	0.57	n.d.	1.8 (0.2–17)	0.33
Atipamezole	4.1 (2.0–9.0)	0.92	5.3 (4.8–8.3)	0.82	n.d.	10 (5.0–23)	1.16
Idazoxan	71 (20–251)	0.71	48 (21–110)	0.73	n.d.	18 (12–34)	0.89
Rauwolscine	0.47 (0.21–1.2)	0.83	0.27 (0.12–0.63)	0.78	n.d.	0.39 (0.20–0.83)	1.14

The apparent K_i (nM) and their 95% confidence intervals from three to six independent experiments, analysed using a one-site competition model. The pseudo-Hill slope (n_H) was obtained using a variable slope model. Receptors are named based on the exchanged domains (see Figure 1). Statistical significances are shown with symbols (one) $P < 0.05$; (two) $P < 0.01$; (three) $P < 0.001$. (a) chimaera versus wild-type α_{2A}; (b) wild-type α_{2A} versus wild-type α_{2B}; (c) wild-type α_{2B} versus wild-type α_{2C}; (d) wild-type α_{2A} versus wild-type α_{2C}.

more reliable molecular models of the α_2-adrenoceptors than the bovine rhodopsin structure.

The TM regions of the β_2-adrenoceptor structure are, nonetheless, well conserved in comparison with the rhodopsin structure: the Cα atoms of the TM helices of the β_2-adrenoceptor structure can be superimposed on those of rhodopsin with a root mean square deviation (RMSD) of 3.9 Å (Cherezov *et al.*, 2007). All of the amino acid positions that were predicted to face the binding cavity in the rhodopsin-based α_2-adrenoceptor models are indeed positioned there in the β_2-adrenoceptor-based ones, too (Figure 3). For example, the key determinants of agonist binding, D3.32, W6.48, S5.43 and S5.46, are well positioned to interact with the protonated nitrogen, aromatic ring, and catecholic hydroxyls of catecholamine agonists. In the β_2-adrenoceptor structure, along the TM1-TM5 axis, TM5 is located closer to the centre of the

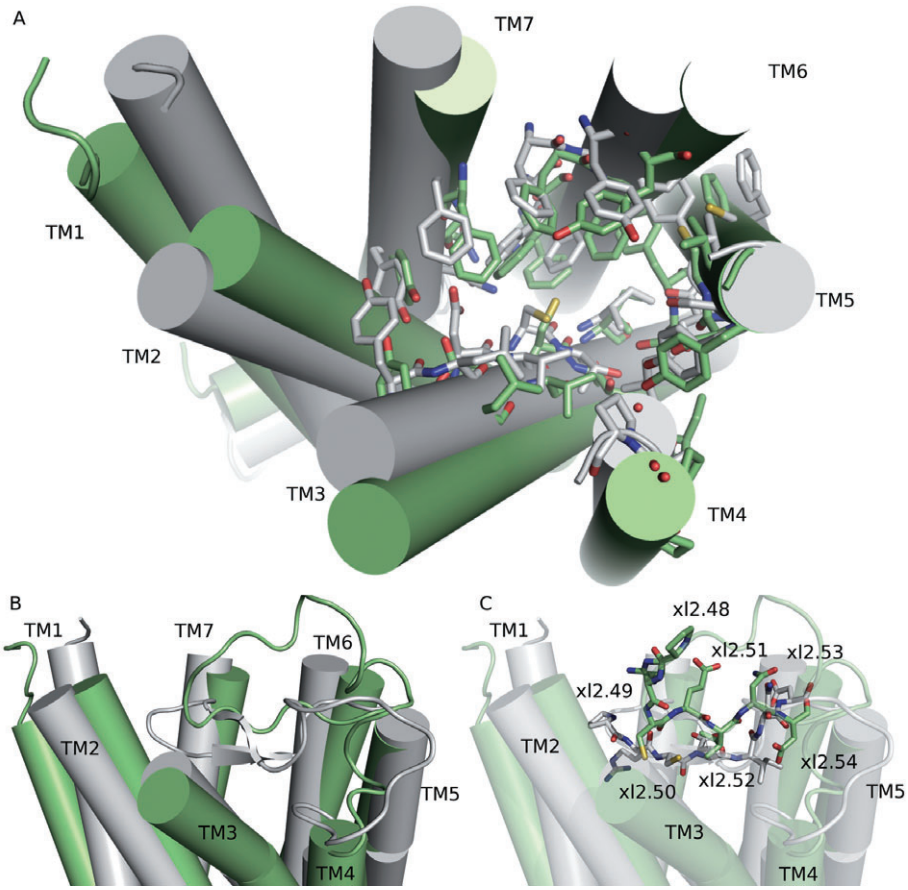

Figure 3

Comparison of molecular models of the α_{2A}-adrenoceptor subtype based on either bovine rhodopsin (grey) or the β_2-adrenoceptor (green) as template. (A) Amino acids of the TM helices were globally well positioned in the rhodopsin-based model. For clarity, not all amino acids that face the binding cavity are shown. Extracellular loop 2 forms the top of the binding pocket and is quite different in rhodopsin-based models (grey) and β_2-adrenoceptor based models (green) (B and C). (B) The general structure of XL2, viewed from the plane of the membrane. (C) Close-up view of positions xl2.48–xl2.54. In (B and C), the view has been tilted by about 70° compared with A.

binding cavity by about 2 Å in comparison to the rhodopsin structure, and this is reflected in our current models of the α_2-adrenoceptors. The distance between the Cα carbon of residue 3.32 and the Cα carbon of residue 5.42 is 12 Å in the β_2-adrenoceptor, ~12.5 Å in our α_2-adrenoceptor models, and 14.5 Å in rhodopsin. The distance along the axis of the cavity that runs from TM3 to TM6 is slightly longer in the β_2-adrenoceptor structure than in rhodopsin, leading to a wider cavity. The distance between the Cα carbons of residues 3.32 and 6.52 is 12.5 Å in the rhodopsin structure and 13.5 Å in the β_2-adrenoceptor structure and the α_2-adrenoceptor models. Also, the TM1–TM5 distance is about 23.5 Å in rhodopsin and 26.5 Å in the adrenoceptors (Figure 3A).

The cysteine at position xl2.50 has similar roles in the β_2-adrenoceptor and in rhodopsin, forming a disulphide bond with the cysteine at position 3.50 and constraining XL2 to fold on top of the binding cavity. In the β_2- and β_1-adrenoceptor structures (Cherezov *et al.*, 2007; Warne *et al.*, 2008), XL2 forms a hairpin that contains an α-helical segment (residues H150 to A158) and a second internal disulphide bridge between C184 (xl2.43) and C190 (xl2.49) that is not present in the α_2-adrenoceptor subtypes or in rhodopsin. In the β_2-adrenoceptor structure, the segment of XL2 that lines the binding cavity (residues xl2.50 to xl2.53) is located clearly deeper by about 4 Å towards the centre of the binding cavity in comparison to rhodopsin (Figure 3B). Consequently, this segment is also shifted in the α_2-adrenoceptor models versus rhodopsin away from TM5 and towards TM1: e.g. the Cα carbons at positions xl2.52 and Cxl2.50 are shifted towards the extracellular surface by 4.0 Å and 5.8 Å, and towards TM1 by 2.5 Å (Figure 3C).

The differences among the three α_2-adrenoceptor subtypes in the amino acids facing the binding cavity that we have previously reported from the rhodopsin-based models (Laurila *et al.*, 2007) are also found in the present β_2-adrenoceptor-based models: i.e. C/S/C variation at position 5.43 and variation of the portion of XL2 lying on top of the binding cavity, composed of residues xl2.49-xl2.52 (RCEI, QCKL, and QCGL in the A, B and C subtypes, respectively). Nonetheless, as a consequence of the shift of XL2 towards TM1, position xl2.49 is less exposed than previously thought, whereas position xl2.54 (D/Q/D) now also contributes to the binding cavity surface.

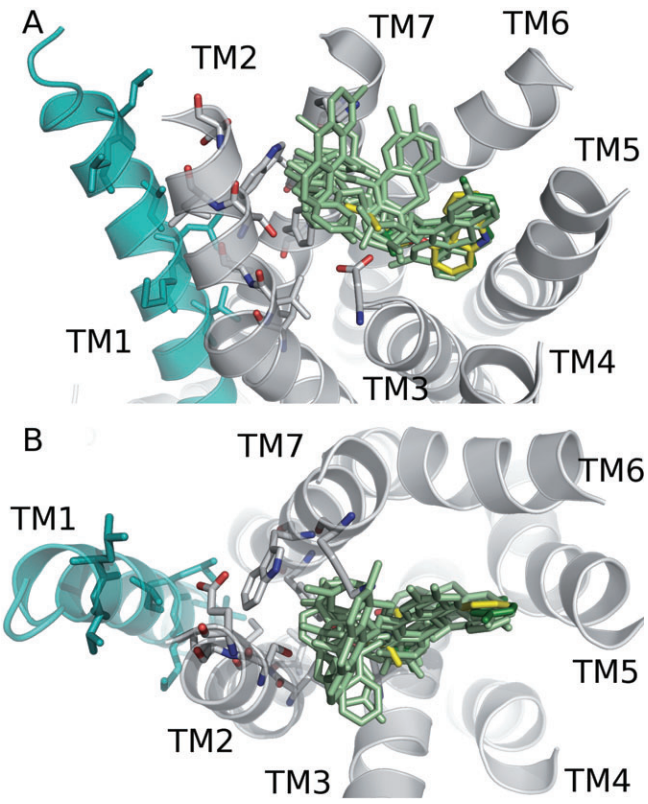

Figure 4

Example of the diversity of ligand positions obtained by automated docking with the programme Gold 4.0, and their distance to TM1 (A) viewed through the membrane plane and (B) rotated by about 70°. In green, all first-ranking positions obtained for chlorpromazine are docked to the ten models of the α_{2A}-adrenoceptor subtype. A similar diversity of positions is observed for the α_{2B}- and α_{2C}-adrenoceptor subtypes (not shown). In yellow, the equivalent location of carazolol is shown in the β_2-adrenoceptor structure. When the positively charged nitrogen of chlorpromazine is at ion pair distance of the negatively charged side-chain oxygen of D3.32, a good superimposition of carazolol is found but the docked molecules do not reach TM1 at the left of the figure (blue). Furthermore, direct contact to TM1 is blocked by side chains from TM2 and TM7 (grey).

Docking of antagonists to the α_2-adrenoceptor model structures

Automated docking was used to investigate possible binding modes at the α_2-adrenoceptors of three antagonists (spiperone, spiroxatrine and chlorpromazine) that showed significant affinity differences in experiments with the chimaeric receptor models (Figures 4 and 5). Rauwolscine was also included in these binding simulations since it has been extensively studied in previous work (Laurila *et al.*, 2007). Docking was performed with each of the ten model structures built for each of the three α_2-adrenoceptor subtypes in order to account for receptor side-chain flexibility (Xhaard *et al.*, 2005). The docked molecules have molecular masses ranging from 354 to 395 g·mol^{-1}, and they all have a centrally located protonated nitrogen atom that has been proposed to form an ion pair with a side-chain oxygen of D3.32.

It is apparent from the docking simulations that all the antagonists investigated, when in contact with D3.32 within the agonist binding site, are too far away from TM1 to form direct contacts with it (Figure 4). Furthermore, access to TM1 from the cavity where agonists are known to bind is occluded by amino acid side chains from TM2 (2.58, 2.61 and 2.65) and TM7 (7.36, 7.40 and 7.43). Another observation from the docking simulations is that there was significant variation in the possible binding modes that were suggested by the docking software (Figure 4). Nonetheless, not all of these binding modes formed the required interaction with D3.32, and many were shifted away from the binding cavity identified in the β_2-adrenoceptor. These different binding modes are not supported by the similarities present in the ligands (compare, e.g. the three-dimensional structures of carazolol and chlorpromazine; see Figure 5) and by the effects of mutations of TM5 on the affinity of rauwolscine (Laurila *et al.*, 2007). Thus, in order to select the most parsimonious binding modes (Figure 5), we used as a criterion the overlap of our ligands with either carazolol or timolol bound to the β_2-adrenoceptor, computed by the programme ShaEP (Vainio *et al.*, 2009). As a result, extremely close superimposition with the poses based on the X-ray structure of the β_2-adrenoceptor was found for the conformations suggested by automated docking of our ligands (Figure 5; see the Supporting information for more detail on docking results). We did not observe subtype-specific clusters of binding modes, which very likely reflects the highly similar binding cavities present in the three α_2-adrenoceptor subtypes and should not be interpreted to imply faults in the theoretical model structures.

Discussion and conclusions

Previously, using site-directed mutagenesis of human and murine α_{2A}-adrenoceptors in combination with molecular models based on the X-ray structure of bovine rhodopsin, we have investigated the effects of mutations in TM5 and XL2 (Laurila *et al.*, 2007). We found that single amino acid substitutions at positions 5.43 and xl2.49-xl2.51 could reverse the inter-species affinity differences of yohimbine, rauwolscine and RS79948-197. The species-specific binding affinities of antagonists with more extended molecular structures were not affected by these mutations, indicating that other residues were influencing their binding affinities. Based on this observation, and by the much lesser sequence conservation of TM1 compared with the other TMs, TM1 was suspected of having an influence on the binding affinity of some large antagonist ligands.

Involvement of TM1 in ligand binding

We prepared eight chimaeric α_2-adrenoceptor constructs: six in the first stage of the study where TM1 and the preceding N-terminal sequence were exchanged between the subtypes, and in the second stage of the study, two chimaeras where only TM1 was exchanged in order to discriminate between any effects due to the N-terminus and TM1. The result was a significant gain of binding affinity for the α_{2A}-adrenoceptor subtype as regards three of the five ligands that had relatively low affinity for this receptor subtype; for the remaining two antagonists, a similar but statistically non-significant trend was observed. No reciprocal effects were seen in the receptor

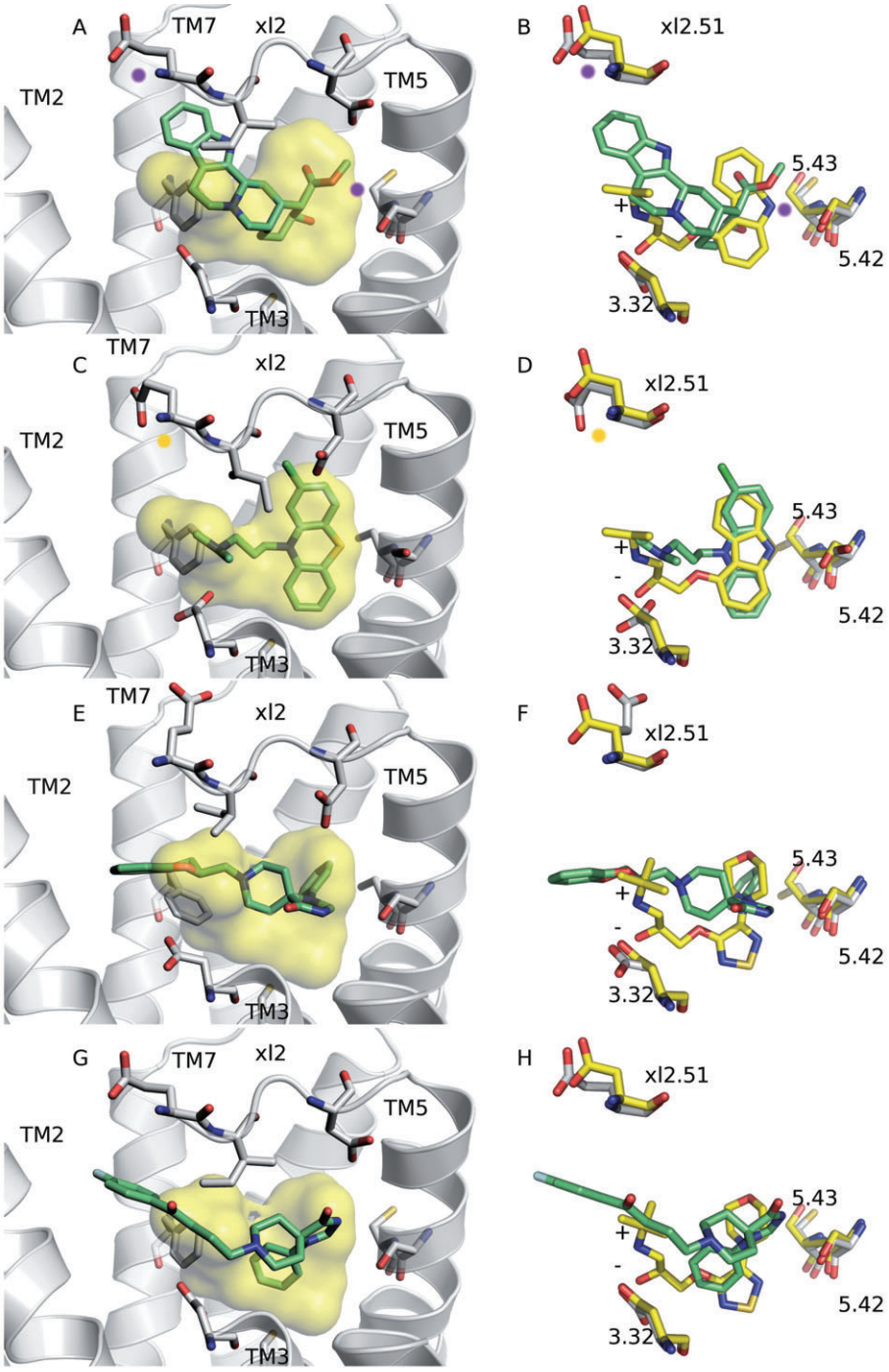

Figure 5

Close-up view of the 'best' positions obtained by automated docking of rauwolscine (A, B), chlorpromazine (C, D), spiroxatrine (E, F) and spiperone (G, H) to the α_{2A}-adrenoceptor model. The poses were ranked according to the shape and electrostatic overlap on the most similar ligand in the β_2-adrenoceptor, either carazolol (rauwolscine, chlorpromazine) or timolol (spiroxatrine, spiperone), using the programme ShaEP (Vainio *et al.*, 2009; see Supporting information). Left panels (A, C, E, G) show the binding site (grey) together with the location of either carazolol or timolol (yellow volumes). Right panels (B, D, F, H) show the actual superimposition of ligands (yellow and green) together with the side chains of D3.32, S5.42, C5.43 and Exl2.51. For spiroxatrine and spiperone (E–H), two alternative orientations were found as described in Xhaard *et al.* 2005. These binding modes are shown in Figure S3.

chimaeras based on the α_{2B}- and α_{2C}-adrenoceptors, where the ligand binding affinities were only marginally affected by the substitutions. In the second stage of the study, we showed that the effects seen for the constructs based on the α_{2A}-adrenoceptor could be ascribed to TM1, and not to the N-terminal segment.

There is some previous experimental evidence from other amine GPCRs for the involvement of TM1 in ligand binding. For the histamine H_1-receptor, two amino acids in TM1, L1.35 and L1.39, have been proposed to participate in the binding of dimeric histaprodifen (Strasser *et al.*, 2008a). For a closer homologue of the α_2-adrenoceptors, the dopamine D_2 receptor, the substituted cysteine accessibility method has been used to demonstrate that six amino acids in TM1 (A1.36, G1.49, N1.50, V1.53, A1.56 and V1.57) are at least transiently accessible to ligands (Shi *et al.*, 2001), whereas in rhodopsin, two amino acids in TM1 (G1.49 and N1.50) were predicted to be accessible in the binding pocket (Shi *et al.*, 2001). Thus, in the α_2-adrenoceptors, TM1 could also be accessible to ligands that enter the binding cavity, even if simultaneous binding to TM3 and TM1 now appears unlikely.

Docking site and accessibility of TM1

Most available experimental evidence suggests that antagonists bind at least in part within the same pocket where agonists bind in α_2-adrenoceptors and related receptors: ligands that form ion-pairs with D3.32 need to fit into an equivalent of the orthosteric pocket close to TM5. The β_1- and β_2-adrenoceptor structures were determined in complex with three ligands (carazolol, cyanopindolol and timolol) relatively similar to ours that all bind within the orthosteric pocket (Cherezov *et al.*, 2007; Hanson *et al.*, 2008; Warne *et al.*, 2008). Phenoxybenzamine, which binds covalently to α_1- and α_2-adrenoceptors, has been shown to attach within the orthosteric site (Frang *et al.*, 2001; Xhaard *et al.*, 2005). For yohimbine analogues, contacts with TM5, TM7 and xl2.49-xl2.51 have been experimentally demonstrated (Suryanarayana *et al.*, 1991; Laurila *et al.*, 2007); direct interactions with TM1 are not likely since TM1 is so far away from TM5. Other experimental evidence based on site-directed mutagenesis also points to the orthosteric pocket as the binding location of antagonists in both α_1-adrenoceptors and 5-HT receptors that are structurally related to α_2-adrenoceptors (Zhao *et al.*, 1996; Wurch *et al.*, 1998).

The presently employed α_2-adrenoceptor models were constructed based on sequence identity of 37–43% with the β_2-adrenoceptor template and should be more accurate than our previous models based on bovine rhodopsin. Nonetheless, one should be aware that molecular receptor models may have inaccuracies resulting from the evolutionary divergence between the modelled structure and the template, as well as errors introduced during the modelling procedure. Generally, molecular models of GPCRs are relatively accurate in the TM regions whereas the extracellular and cytoplasmic loop domains are more difficult to model (Michino *et al.*, 2009). Furthermore, molecular models represent only static views of receptors that are flexible entities in cells. Nonetheless, in the present case, the β_2-adrenoceptor that was used as the model template was bound to the partial inverse agonist carazolol (Cherezov *et al.*, 2007) that, in light of current knowledge, should be optimal for building reasonable molecular models of the α_2-adrenoceptors in complex with antagonist ligands.

As such, our molecular models suggest very limited exposure of TM1 to the binding pocket, as TM1 is distant from the orthosteric binding cavity. Since the TM1–TM5 distance now is longer than in previous rhodopsin-based models (Figure 3) (26.5 Å in the β_2-adrenoceptor vs. 23.5 Å in rhodopsin), small-molecule ligands that occupy the agonist (orthosteric) site close to TM5 cannot simultaneously be in contact with TM1. Furthermore, access to TM1 is blocked by side-chain atoms from TM2 and TM7 (Figure 4). We propose that the β_2-adrenoceptor structure should be used to re-assess other docking simulation studies that have reported TM1 binding in amine receptors in addition to contacts with the conserved D3.32 in TM3. Such predictions include, for example, three residues (Y1.39, L1.42 and I1.43) in TM1 of the dopamine D_2 receptor that were proposed to bind spiperone (Boeckler *et al.*, 2005) and three aliphatic residues in TM1 that were suggested to contribute to the binding cavity in a chemogenomic analysis of the amine GPCR family (Surgand *et al.*, 2006).

Molecular docking to β_2-adrenoceptor-based models

That rauwolscine binds in the orthosteric pocket of α_2-adrenoceptors has by now been confirmed by several site-directed mutagenesis studies. In addition to ion-pairing with 3.32, direct contacts have been suggested at positions 7.39 and 5.43. Experimental results from substitution of F7.39 with an asparagine and of C5.43 with a serine show increased binding affinity of yohimbine at the human α_{2A}-adrenoceptor (Suryanarayana *et al.*, 1991; Cockcroft *et al.*, 2000). In addition, we have previously shown that substitutions at xl2.49 and xl2.51 significantly and reciprocally affect the binding of rauwolscine (Laurila *et al.*, 2007). In our new molecular models based on the β_2-adrenoceptor, together with xl2.50 and xl2.52, position xl2.51 forms the aromatic 'lid' of the binding pocket. When comparing the automated docking of the extended structures of chlorpromazine, spiperone and spiroxatrine to that of the more curved rauwolscine, only rauwolscine comes into close contact with the side chain of xl2.51 (Figure 5). This supports the suggested binding modes as it provides a structural explanation for our previously observed effects of the side chains of XL2 to the binding of yohimbine but not chlorpromazine, spiperone and spiroxatrine.

The side chain of xl2.51 is, however, facing away from the binding cavity. In the β_2-adrenoceptor structure, the carboxyl group of D192 (xl2.51) forms a salt bridge with a positively charged lysine (K7.32) in TM7. The amino acids in the α_2-adrenoceptors at equivalent positions are in the α_{2A}-adrenoceptor Exl2.51 and R7.32, in the α_{2B}-adrenoceptor Kxl2.51 and H7.32 and two glycines at positions xl2.51 and 7.32 in the α_{2C}-adrenoceptor. Ligands, by affecting this interaction, may have allosteric effects, as recently reported for the β_2-adrenoceptor (Bokoch *et al.*, 2010). An important earlier study that used the rhodopsin activation mechanism (Robinson *et al.*, 1992) as a starting point had, furthermore, shown that exchange of the positively charged K7.32 to A (neutral) or E (negatively charged) in the α_{1B}-adrenoceptor increased

the binding affinity of noradrenaline and adrenaline, suggesting this ion-pair interaction to be important for the resting receptor conformation (Porter *et al.*, 1996). Thus, the indirect effects that we observed in this study, as well as the effects of XL2 mutations on the binding of yohimbine analogues (Laurila *et al.*, 2007), may be mediated by this ionic interaction between XL2 and TM7 in the α_{2A}-adrenoceptor subtype. This positively charged arginine (R7.32) in TM7 of the human α_{2A}-adrenoceptor has so far not been subjected to mutagenesis experiments.

An effect on binding does not necessarily imply direct atomic contact

Our experimental results show that TM1 contributes to the binding properties of some large antagonist ligands at the α_{2A}-adrenoceptor, but reciprocal effects were not seen for α_{2B}- and α_{2C}-adrenoceptors. Binding affinity is, however, determined by more factors than the direct interactions of the ligand and the receptor (approximated by the enthalpic component), as it also includes the dynamics of different segments of the receptor and the loss of flexibility upon ligand binding (approximated by the entropic component) (Wittmann *et al.*, 2009). Other factors that have been discussed include the presence of charged groups even outside of the pocket that affect the pK_a and hence the protonation state of compounds; the charged side chains do indeed differ between the α_2-adrenoceptor subtypes in the vicinity of the binding pocket. Side chains along TM1 may influence the packing of side chains on other TMs that pack against it and hence may affect the overall shape of the binding pocket. Thus, some regions outside of the orthosteric binding pocket may very well be involved in ligand binding specificity without direct contacts and direct effects on the binding pose. For example, from a recent structural analysis of the histamine H_1 receptor it has been proposed that its N-terminus may contribute indirectly to the pharmacological properties of certain types of ligands by indirect interactions with the second extracellular loop (Strasser *et al.*, 2008b). Also, three TM6 amino acids facing away from the cavity, and several residues in the third intracellular loop of the melanocortin receptors MC_1 and MC_4 were, in a mutagenesis study, identified to account for most of the subtype difference in the affinity for α-MSH (Prusis *et al.*, 2006).

Concluding remarks

We have experimentally demonstrated that TM1 is involved in determining the subtype-specific antagonist binding profile of the α_{2A}-adrenoceptor subtype. Our improved α_2-adrenoceptor models based on the β_2-adrenoceptor structural template suggest that ligands cannot bind simultaneously in the agonist binding pocket between TM3 and TM5 and be in direct contact with TM1. Furthermore, molecular modelling of the α_2-adrenoceptors suggests very similar binding cavities in the A, B and C subtypes. Such highly similar cavities would be expected to accommodate ligands in a similar manner. Thus, the pharmacological effects of the mutations introduced in this study are best explained by indirect effects. A better understanding of such effects may provide input into the design of highly subtype-selective new drugs.

Acknowledgements

Dr Saku Ruohonen, PhD, is thanked for his guidance in reverse transcription PCR. Ms Ulla Uoti is gratefully acknowledged for skilful technical assistance. This study was supported by grants from the Finnish Society of Sciences and Letters, Orion-Farmos Research Foundation, Ida Montin Foundation, the Academy of Finland, the Sigrid Jusélius Foundation, the Åbo Akademi Center of Excellence Program in Cell Stress, the Joe, Pentti and Tor Borg Foundation, the ERASMUS program of the European Union and DDGS – the Drug Discovery Graduate School.

Conflicts of interest

MS has received speaker's fees and consultation fees from Orion Corporation, a pharmaceutical company with an active α_2-adrenoceptor programme. He has also contract research relationships with Orion Corporation. JOR has received speaker's fees from Orion Corporation.

References

Altman JD, Trendelenburg AU, MacMillan L, Bernstein D, Limbird L, Starke K *et al.* (1999). Abnormal regulation of the sympathetic nervous system in alpha2A-adrenergic receptor knockout mice. Mol Pharmacol 56: 154–161.

Ballesteros JA, Weinstein H (1995). Integrated methods for the construction of three-dimensional models and computational probing of structure-function relations in G protein-coupled receptors. In: Sealfon SC (ed.). Receptor Molecular Biology. Academic Press Inc: San Diego, CA, pp. 366–427.

Boeckler F, Lanig H, Gmeiner P (2005). Modeling the similarity and divergence of dopamine D2-like receptors and identification of validated ligand-receptor complexes. J Med Chem 48: 694–709.

Bokoch MP, Zou Y, Rasmussen SG, Liu CW, Nygaard R, Rosenbaum DM *et al.* (2010). Ligand-specific regulation of the extracellular surface of a G-protein-coupled receptor. Nature 463: 108–112.

Bradford MM (1976). A rapid and sensitive method for the quantitation of microgram quantities of protein utilizing the principle of protein-dye binding. Anal Biochem 7: 248–254.

Brede M, Wiesmann F, Jahns R, Hadamek K, Arnolt C, Neubauer S *et al.* (2002). Feedback inhibition of catecholamine release by two different alpha2-adrenoceptor subtypes prevents progression of heart failure. Circulation 106: 2491–2496.

Cheng Y, Prusoff WH (1973). Relationship between the inhibition constant (Ki) and the concentration of inhibitor which causes 50 per cent inhibition (I50) of an enzymatic reaction. Biochem Pharmacol 22: 3099–3108.

Cherezov V, Rosenbaum DM, Hanson MA, Rasmussen SG, Thian FS, Kobilka TS *et al.* (2007). High-resolution crystal structure of an engineered human beta2-adrenergic G protein-coupled receptor. Science 318: 1258–1265.

Cockcroft V, Frang H, Pihlavisto M, Marjamäki A, Scheinin M (2000). Ligand recognition of serine-cysteine amino acid exchanges in transmembrane domain 5 of alpha2-adrenergic receptors by UK 14,304. J Neurochem 74: 1705–1710.

Deupree JD, Hinton KA, Cerutis DR, Bylund DB (1996). Buffers differentially alter the binding of [^{3}H]rauwolscine and [^{3}H]RX821002 to the alpha-2 adrenergic receptor subtypes. J Pharmacol Exp Ther 278: 1215–1227.

Eason MG, Jacinto MT, Theiss CT, Liggett SB (1994). The palmitoylated cysteine of the cytoplasmic tail of alpha 2A-adrenergic receptors confers subtype-specific agonist-promoted downregulation. Proc Natl Acad Sci USA 91: 11178–11182.

Frang H, Cockcroft V, Karskela T, Scheinin M, Marjamäki A (2001). Phenoxybenzamine binding reveals the helical orientation of the third transmembrane domain of adrenergic receptors. J Biol Chem 276: 31279–31284.

Halme M, Sjöholm B, Savola JM, Scheinin M (1995). Recombinant human alpha 2-adrenoceptor subtypes: comparison of [^{3}H]rauwolscine, [^{3}H]atipamezole and [^{3}H]RX821002 as radioligands. Biochim Biophys Acta 1266: 207–214.

Hanson MA, Cherezov V, Griffith MT, Roth CB, Jaakola VP, Chien EY *et al.* (2008). A specific cholesterol binding site is established by the 2.8 Å structure of the human beta2-adrenergic receptor. Structure 16: 897–905.

Hein L, Kobilka BK (1995). Adrenergic receptor signal transduction and regulation. Neuropharmacology 34: 357–366.

Hein L, Altman JD, Kobilka BK (1999). Two functionally distinct alpha2-adrenergic receptors regulate sympathetic neurotransmission. Nature 402: 181–184.

Jaakola VP, Griffith MT, Hanson MA, Cherezov V, Hien EY, Lane JR *et al.* (2008). The 2.6 angstrom crystal structure of a human A2A adenosine receptor bound to an antagonist. Science 322: 1211–1217.

Johnson MS, Overington JP (1993). A structural basis for sequence comparisons. An evaluation of scoring methodologies. J Mol Biol 233: 716–738.

Jones G, Willett P, Glen RC, Leach AR, Taylor R (1997). Development and validation of a genetic algorithm for flexible docking. J Mol Biol 267: 727–748.

Laurila JM, Xhaard H, Ruuskanen JO, Rantanen MJ, Karlsson HK, Johnson MS *et al.* (2007). The second extracellular loop of alpha2A-adrenoceptors contributes to the binding of yohimbine analogues. Br J Pharmacol 151: 1293–1304.

Link RE, Desai K, Hein L, Stevens ME, Chruscinski A, Bernstein D *et al.* (1996). Cardiovascular regulation in mice lacking alpha2-adrenergic receptor subtypes b and c. Science 273: 803–805.

MacDonald E, Scheinin M (1995). Distribution and pharmacology of alpha2-adrenoceptors in the central nervous system. J Physiol Pharmacol 46: 241–258.

MacDonald E, Kobilka BK, Scheinin M (1997). Gene targeting – homing in on alpha2-adrenoceptor-subtype function. Trends Pharmacol Sci 18: 211–219.

MacMillan LB, Hein L, Smith MS, Piascik MT, Limbird LE (1996). Central hypotensive effects of the alpha2a-adrenergic receptor subtype. Science 273: 801–803.

Mansouri J, Panigrahy A, Assmann SF, Kinney HC (2001). Distribution of alpha2-adrenergic receptor binding in the developing human brain stem. Pediatr Dev Pathol 4: 222–236.

Marjamäki A, Frang H, Pihlavisto M, Hoffrén AM, Salminen T, Johnson MS *et al.* (1999). Chloroethylclonidine and 2-aminoethyl methanethiosulfonate recognize two different conformations of the human alpha(2A)-adrenergic receptor. J Biol Chem 274: 21867–21872.

Michino M, Abola E, GPCR Dock 2008 participants, Brooks CL 3rd, Dixon JS, Moult J, Stevens RC (2009). Community-wide assessment of GPCR structure modelling and ligand docking: GPCR Dock 2008. Nat Rev Drug Discov 8: 455–463.

Palczewski K, Kumasaka T, Hori T, Behnke CA, Motoshima H, Fox BA *et al.* (2000). Crystal structure of rhodopsin: a G protein-coupled receptor. Science 289: 739–745.

Peltonen JM, Nyrönen T, Wurster S, Pihlavisto M, Hoffrén AM, Marjamäki A *et al.* (2003). Molecular mechanisms of ligand-receptor interactions in transmembrane domain V of the alpha2A-adrenoceptor. Br J Pharmacol 140: 347–358.

Pohjanoksa K, Jansson CC, Luomala K, Marjamäki A, Savola JM, Scheinin M (1997). Alpha2-adrenoceptor regulation of adenylyl cyclase in CHO cells: Dependence on receptor density, receptor subtype and current activity of adenylyl cyclase. Eur J Pharmacol 335: 53–63.

Porter JE, Hwa J, Perez DM (1996). Activation of the alpha1b-adrenergic receptor is initiated by disruption of an interhelical salt bridge constraint. J Biol Chem 271: 28318–28323.

Prusis P, Uhlén S, Petrovska R, Lapinsh M, Wikberg JE (2006). Prediction of indirect interactions in proteins. BMC Bioinformatics 7: 167.

Robinson PR, Cohen GB, Zhukovsky EA, Oprian DD (1992). Constitutively active mutants of rhodopsin. Neuron 4: 719–725.

Rosenbaum DM, Cherezov V, Hanson MA, Rasmussen SG, Thian FS, Kobilka TS *et al.* (2007). GPCR engineering yields high-resolution structural insights into beta2-adrenergic receptor function. Science 318: 1266–1273.

Ruffolo RR, Hieble JP (1994). Alpha-adrenoceptors. Pharmacol Ther 61: 1–64.

Ruuskanen JO, Xhaard H, Marjamäki A, Salaneck E, Salminen T, Yan YL *et al.* (2004). Identification of duplicated fourth alpha2-adrenergic receptor subtype by cloning and mapping of five receptor genes in zebrafish. Mol Biol Evol 21: 14–28.

Ruuskanen JO, Laurila J, Xhaard H, Rantanen VV, Vuoriluoto K, Wurster S *et al.* (2005). Conserved structural, pharmacological and functional properties among the three human and five zebrafish alpha 2-adrenoceptors. Br J Pharmacol 144: 165–177.

Sali A, Blundell TL (1993). Comparative protein modelling by satisfaction of spatial restraints. J Mol Biol 234: 779–815.

Saunders C, Limbird LE (1999). Localization and trafficking of alpha2-adrenergic receptor subtypes in cells and tissues. Pharmacol Ther 84: 193–205.

Scheinin M, Lomasney JW, Hayden-Hixson DM, Schambra UB, Caron MG, Lefkowitz RJ *et al.* (1994). Distribution of alpha2-adrenergic receptor subtype gene expression in rat brain. Brain Res Mol Brain Res 21: 133–149.

Shi L, Simpson MM, Ballesteros JA, Javitch JA (2001). The first transmembrane segment of the dopamine D2 receptor: Accessibility in the binding-site crevice and position in the transmembrane bundle. Biochemistry 40: 12339–12348.

Strader CD, Sigal IS, Register RB, Candelore MR, Rands E, Dixon RA (1987). Identification of residues required for ligand binding to the beta-adrenergic receptor. Proc Natl Acad Sci USA 84: 4384–4388.

Strader CD, Candelore MR, Hill WS, Sigal IS, Dixon RA (1989). Identification of two serine residues involved in agonist activation of the beta-adrenergic receptor. J Biol Chem 264: 13572–13578.

Strasser A, Striegl B, Wittmann HJ, Seifert R (2008a). Pharmacological profile of histaprodifens at four recombinant histamine H1 receptor species isoforms. J Pharmacol Exp Ther 324: 60–71.

Strasser A, Wittmann HJ, Seifert R (2008b). Ligand-specific contribution of the N terminus and E2-loop to pharmacological properties of the histamine H1-receptor. J Pharmacol Exp Ther 326: 783–791.

Surgand JS, Rodrigo J, Kellenberger E, Rognan D (2006). A chemogenomic analysis of the transmembrane binding cavity of human G-protein-coupled receptors. Proteins 62: 509–538.

Suryanarayana S, Daunt DA, Von Zastrow M, Kobilka BK (1991). A point mutation in the seventh hydrophobic domain of the alpha 2-adrenergic receptor increases its affinity for a family of beta receptor antagonists. J Biol Chem 266: 15488–15492.

Uhlén S, Dambrova M, Näsman J, Schiöth HB, Gu Y, Wikberg-Matsson A *et al.* (1998). [^{3}H]RS79948-197 binding to human, rat, guinea pig and pig alpha2A-, alpha2B- and alpha2C-adrenoceptors. Comparison with MK912, RX821002, rauwolscine and yohimbine. Eur J Pharmacol 343: 93–101.

Vainio MJ, Puranen JS, Johnson MS (2009). ShaEP: molecular overlay based on shape and electrostatic potential. J Chem Inf Model 49: 492–502.

Wang CD, Buck MA, Fraser CM (1991). Site-directed mutagenesis of alpha2A-adrenergic receptors: Identification of amino acids involved in ligand binding and receptor activation by agonists. Mol Pharmacol 40: 168–179.

Warne T, Serrano-Vega MJ, Baker JG, Moukhametzianov R, Edwards PC, Henderson R *et al.* (2008). Structure of a beta1-adrenergic G-protein-coupled receptor. Nature 454: 486–491.

Weis WI, Kobilka BK (2008). Structural insights into G-protein-coupled receptor activation. Curr Opin Struct Biol 18: 734–740.

Wittmann HJ, Seifert R, Strasser A (2009). Contribution of binding enthalpy and entropy to affinity of antagonist and agonist binding at human and guinea pig histamine H(1)-receptor. Mol Pharmacol 76: 25–37.

Wurch T, Colpaert FC, Pauwels PJ (1998). Chimeric receptor analysis of the ketanserin binding site in the human 5-hydroxytryptamine1D receptor: importance of the second extracellular loop and fifth transmembrane domain in antagonist binding. Mol Pharmacol 56: 1088–1096.

Xhaard H, Nyrönen T, Rantanen VV, Ruuskanen JO, Laurila J, Salminen T *et al.* (2005). Model structures of alpha-2 adrenoceptors in complex with automatically docked antagonist ligands raise the possibility of interactions dissimilar from agonist ligands. J Struct Biol 150: 126–143.

Xhaard H, Rantanen VV, Nyrönen T, Johnson MS (2006). Molecular evolution of adrenoceptors and dopamine receptors: Implications for the binding of catecholamines. J Med Chem 49: 1706–1719.

Zhao MM, Hwa J, Perez DM (1996). Identification of critical extracellular loop residues involved in alpha 1-adrenergic receptor subtype-selective antagonist binding. Mol Pharmacol 50: 1118–1126.

Supporting information

Additional Supporting Information may be found in the online version of this article:

Figure S1 Multiple sequence alignment of the three human α2-adrenoceptor subtypes indicating the predicted secondary structure and boundaries of the TM helices as derived from bovine rhodopsin and the β2-adrenoceptor X-ray structures. A multiple sequence alignment of the α2-adrenoceptors with β2-adrenoceptor and rhodopsin was first constructed to build the figure (not shown). The secondary structures are as reported in the PDB files and are displayed on top of the alignments for the β2-adrenoceptor (PDB 2RH1) and rhodopsin (PDB 1U19): cylinders indicate α-helical domains and arrows β-strands. The amino acids of the orthosteric binding site are indicated with an (*) above the respective secondary structure elements and were defined as having at least one atom within 5 Å of the ligand, either carazolol or retinal. Amino acids conserved among the three α2-adrenoceptor subtypes are highlighted in dark grey. Amino acids forming the third intracellular loop are highlighted in light gray.

Figure S2 Top. Ranking of docked poses using a shape similarity index computed by the programme ShaEP (Vainio *et al.*, 2009). Similarity is measured between chlorpromazine, rauwolscine, spiroxatrine and spiperone docked to the 10 molecular models of each α2-adrenoceptor subtype, and carazolol (chlorpromazine and rauwolscine) or timolol (spiroxatrine and spiperone) bound to the β2-adrenoceptor. The TM regions of the β2-adrenoceptor were first superimposed with the equivalent region of each of the α2-adrenoceptor models in order to position carazolol or timolol into the α2-adrenoceptor models. The 'best' scores were assigned to poses with the highest molecular overlap on timolol or carazolol (see the dark green and yellow molecules in Figure 4 of the article). The maximum similarity ranges between 0 (no overlap) and, since the ligands differ, a value less than 1: 0.70 (maximum similarity computed between rauwolscine and carazolol when the superposition is optimized by the ShaEP genetic algorithm), 0.80 (chlorpromazine-carazolol), 0.67 (spiroxatrine-timolol) and 0.66 (spiperone-timolol). Only the similarity in molecular shape is reported, as the electrostatic similarity is difficult to interpret. Bottom. For comparison, the equivalent docking scores as computed by Goldscore are also given and show that there is no correlation between the Goldscore and the ranking according to ShaEP.

Figure S3 Alternative binding modes observed for spiroxatrine (A, B) and spiperone (C, D) docked into the α2A-adrenoceptor model. Left panels (A, C) show the binding site (grey) together with the location of timolol (yellow volumes). Right panels (B, D) show the actual superimposition of ligands (yellow and grey) together with the side chains of D3.32, S5.42, C5.43 and Exl2.51. These orientations complement Figure 5.

Table S1 A list of primers used for mutagenesis and RT-PCR. Nucleotides that encode an artificial restriction enzyme recognition site or mutation are highlighted with colour: *Kpn*I (blue), *Spe*I (red), *Hin*dIII (green) and mutation (bold black)

Table S2 Numerical values used to draw Figure S2

Table S3 Key distances between functional groups of docked chlorpromazine, rauwolscine, spiroxatrine or spiperone as compared with carazolol or timolol bound to the β2-adrenoceptor when the TM region of the β2-adrenoceptor is superimposed to the equivalent region of each of the α2-adrenoceptor models. The functional groups compared are annotated as follows: N^+/N^+, distances measured between

the protonated amine of carazolol or timolol and the protonated amine of chlorpromazine, rauwolscine or spiroxatrine; N^+/OH, distances measured between the –OH group of carazolol or timolol and the protonated amine of chlorpromazine, rauwolscine or spiroxatrine; -$N^=$/S or -$N^=$/OH distances measured between the cyclic nitrogen atom of carazolol and the sulphur atom of chlorpromazine or the hydroxyl group of rauwolscine; –S^-/N distances between the sulphur atom of timolol and the cyclic nitrogen of spiroxatrine and spiperone. Distances are only given for the three most similar complexes, as computed by ShaEP

Table S4 Key distances between functional groups of docked ligands and specified amino acids of the α2-adrenoceptor models. For D3.32, distances are measured from the closest side-chain carboxylate oxygen of D3.32 to the protonated amine of ligands; for S5.42, distances are measured from the side-chain hydroxyl to the –OH of rauwolscine or the sulphur of chlorpromazine or the ring nitrogen of spiroxatrine or spiperone; otherwise, the distances are shown for the closest approaching atom between the amino acid and the ligand. Distances are only given for the three most similar complexes as computed by ShaEP

Table S5 Distances (Å) between D3.32 and the protonated amine of chlorpromazine, rauwolscine, spiroxatrine and spiperone. Models are ranked according to their ShaEP scores

Please note: Wiley-Blackwell are not responsible for the content or functionality of any supporting materials supplied by the authors. Any queries (other than missing material) should be directed to the corresponding author for the article.